Note: This copy is for your personal, non-commercial use only. To order presentation-ready copies for distribution to your colleagues or clients, contact us at www.rsna.org/rsnarights.

Ligaments and Plicae of the Elbow: Normal MR Imaging Variability in 60 Asymptomatic Subjects[1]

Daniela B. Husarik, MD
Nadja Saupe, MD
Christian W. A. Pfirrmann, MD
Bernhard Jost, MD
Juerg Hodler, MD, MBA
Marco Zanetti, MD

Purpose: To prospectively evaluate the normal variability of ligaments, plicae, and the posterior capitellum on conventional magnetic resonance (MR) images of the elbow in asymptomatic volunteers.

Materials and Methods: The study was approved by the institutional ethics board, and informed consent was obtained from all subjects. MR imaging was performed at 1.5 T in 60 asymptomatic volunteers (30 women, 30 men; age range, 22–51 years; median age, 32.8 years) by using the following five pulse sequences: transverse T1-weighted spin-echo, sagittal T2-weighted fast spin-echo, coronal fast spin-echo short-inversion-time inversion recovery, transverse intermediate-weighted with fat saturation, and coronal three-dimensional water-excitation true fast imaging with steady-state precession. The visibility (completely visible over the entire course, partially visible, or not visible) and signal intensity characteristics (hypointense or hyperintense to muscle, homogeneous signal intensity vs striation) of the elbow ligaments and plicae were evaluated by three independent readers. The presence of pseudodefects at the posterior capitellum was determined. The dimensions of all structures were measured by two independent readers.

Results: The anterior ulnar collateral ligament (UCL) and radial collateral ligament (RCL) were visible over their entire course in all 60 subjects (100%). The posterior UCL, lateral UCL, and annular ligament (AL) were completely visible in 58 (97%), 51 (85%), and 59 (98%) of the 60 subjects, respectively, and partially visible in the remaining subjects. Increased signal intensity with fluid-sensitive sequences was found in the anterior UCL in nine of the 60 subjects (15%), posterior UCL in four subjects (7%), RCL in one subject (2%), lateral UCL in six subjects (10%), and AL in one subject (2%). The median thickness and 90th percentile were 2.5 and 3.5 mm, respectively, for the anterior UCL, 1.0 and 1.7 mm for the posterior UCL, 1.9 and 2.8 mm for the RCL, 2.3 and 3.8 mm for the lateral UCL, and 1.0 and 1.3 mm for the AL. A posterolateral plica (median dimension, 4.3 × 1.9 × 3.9 mm) was found in 59 of the 60 subjects (98%), whereas a posterior plica (median dimension, 1.8 × 1.4 mm) could be detected in only 20 (33%). A pseudodefect of the capitellum was noted in 51 of the 60 subjects (85%).

Conclusion: The elbow ligaments and the posterolateral plica are consistently visible on conventional MR images of asymptomatic subjects. Most normal ligaments are thinner than 4 mm, and most plicae are thinner than 3 mm.

© RSNA, 2010

[1] From the Department of Radiology, University Hospital Zurich, Zurich, Switzerland (D.B.H., N.S., J.H.); and Department of Radiology, University Hospital Balgrist, Zurich, Switzerland (C.W.A.P., B.J., M.Z.). From the 2009 RSNA Annual Meeting. Received November 27, 2009; revision requested January 25, 2010; revision received April 26; accepted May 6; final version accepted May 18. **Address correspondence to** D.B.H., Department of Radiology, Division of Abdominal Imaging, Duke University Medical Center, DUMC 3808, Durham, NC 27701 (e-mail: *danielahusarik@yahoo.com*).

© RSNA, 2010

The ligaments of the elbow consist of the medial collateral ligament complex with three components of the ulnar collateral ligament (UCL)—the anterior UCL, posterior UCL, and transverse bundle—and the lateral collateral ligament complex with the radial collateral ligament (RCL), lateral UCL, and annular ligament (AL) (1–16). Assessment of the ligaments is useful in the evaluation of patients with elbow instability (6). However, some biomechanically important ligaments (eg, the lateral UCL) are not consistently seen on magnetic resonance (MR) images (17) or in dissected specimens of cadavers (11). Specific MR techniques with oblique imaging planes along the lateral UCL have been recommended (4).

It has been suggested that synovial plicae may be responsible for clinical symptoms when detected on MR images (18–21). Several synovial plicae have been described within the elbow joint (18,20), with the posterolateral plica between the radial head and the capitellum (also referred to as the synovial fold of the humeroradial or radiocapitellar joint [20]) being the most frequently identified. Cadaveric studies showed posterolateral synovial folds in 86% of cases (20). The posterior plica can be found at the superior margin of the lateral olecranon recess. Hypertrophic plicae may cause mechanical symptoms of the elbow (18,21). However, an overlap of plica size has been found in symptomatic and asymptomatic elbows (18). Cutoff values for thickened elbow folds (eg, 3 mm) are suggested in the literature but, to our knowledge, have not been confirmed in a larger population (19,21).

The posterolateral plica is in close contact with the capitellum, where a bone groove with an irregular surface produces a pseudodefect by means of an abrupt contour change at the posterolateral margin of the capitellum, at the junction of the capitellum with the lateral epicondyle of the humerus (22).

The pseudodefect of the capitellum must be differentiated from a true osseous and osteochondral lesion such as that seen in Panner disease, osteochondritis dissecans, Osborne-Cotterill lesion, and acute traumatic impaction injuries of the capitellum, in which additional findings (eg, abnormal marrow signal intensity or fracture lines) can be found (23–30).

Therefore, we examined a large group of asymptomatic subjects. The purpose of our study was to prospectively evaluate the normal variability of ligaments, plicae, and the posterior capitellum on conventional MR images of the elbow in asymptomatic subjects.

Advances in Knowledge

- The posterolateral plica is almost always (98% of cases) visible in asymptomatic subjects.
- The ligaments in asymptomatic elbows are usually thinner than 4 mm (90th percentile ranges from 1.3 to 3.8 mm), and plicae are usually thinner than 3 mm.
- The anterior and lateral ulnar collateral ligaments in asymptomatic elbows are often striated (87% and 78% of cases, respectively).

Materials and Methods

Subjects

The study was approved by the institutional review board of University Hospital Balgrist. Informed consent was obtained from each subject. The MR images of 60 asymptomatic volunteers (median age, 32.8 years; age range, 22–51 years), who were previously investigated for another study (31), were prospectively included in this study. There were 30 men (median age, 33.6 years; age range, 22–50 years) and 30 women (median age, 31.5 years; age range, 22–51 years). Ten male and 10 female subjects were included for each decade between 21 and 51 years.

Implication for Patient Care

- Knowledge of the normal dimensions and signal intensity characteristics of the ligaments and plicae in asymptomatic elbows may avoid false-positive diagnoses related to ligaments and synovial plicae.

The height of the volunteers ranged from 150 to 197 cm (median, 173 cm), the weight ranged from 48 to 94 kg (median, 67 kg), and the body mass index ranged from 17.3 to 31.1 (median, 22.9). The elbows of the dominant arm (55 right and five left arms) in all subjects were asymptomatic. A questionnaire was used to ensure that the subjects *(a)* had not previously undergone elbow surgery, *(b)* had no current arm or elbow pain, *(c)* had no paresthesias in the dominant arm, *(d)* had never been to a physician for elbow complaints, *(e)* had no injuries of the dominant elbow, *(f)* had no need to discontinue work or exercise due to elbow pain, and *(g)* had no history of systemic inflammatory disease. The Mayo Elbow Performance score (32)—which is used to assess pain, range of motion, stability, and daily function of elbows—was 100 (the maximum possible) for all subjects, indicating that the elbows were fully functional and asymptomatic.

MR Imaging Protocol

MR imaging was performed with a 1.5-T MR system (Symphony or Avanto; Siemens Medical Solutions, Erlangen, Germany). The subjects were imaged in the prone position, with the dominant arm in full extension above the head and the forearm in pronation. A four-channel phased-array small extremity coil was placed over the elbow joint. T1-weighted spin-echo

Published online before print
10.1148/radiol.10092163

Radiology 2010; 257:185–194

Abbreviations:
AL = annular ligament
FISP = fast imaging with steady-state precession
RCL = radial collateral ligament
STIR = short inversion time inversion recovery
UCL = ulnar collateral ligament

Author contributions:
Guarantors of integrity of entire study, D.B.H., M.Z.; study concepts/study design or data acquisition or data analysis/interpretation, all authors; manuscript drafting or manuscript revision for important intellectual content, all authors; manuscript final version approval, all authors; literature research, D.B.H., M.Z.; clinical studies, all authors; statistical analysis, N.S.; and manuscript editing, D.B.H., C.W.A.P., B.J., J.H., M.Z.

Authors stated no financial relationship to disclose.

images were obtained in the transverse plane (repetition time msec/echo time msec, 475/11; section thickness, 4 mm; gap, 10%; rectangular field of view, 120 × 90 mm; matrix size, 512 × 256; voxel size, 0.4 × 0.2 × 4 mm; one acquisition). T2-weighted fast spin-echo images were obtained in the sagittal plane (3500/88; section thickness, 4 mm; gap, 10%; field of view, 120 × 109 mm; matrix size, 512 × 256; voxel size, 0.4 × 0.2 × 4 mm; two acquisitions). Fast spin-echo short-inversion-time inversion-recovery (STIR) images were obtained in the coronal plane (4100/29; inversion time, 130 msec; section thickness, 3 mm; gap, 10%; field of view, 120 × 109 mm; matrix size, 256 × 209; voxel size, 0.5 × 0.5 × 3 mm; one acquisition). Intermediate-weighted fat-saturated images were obtained in the transverse plane (3000/38; section thickness, 4 mm; gap, 10%; field of view, 512 × 256 mm; matrix size, 384 × 235; voxel size, 0.4 × 0.3 × 4 mm; one acquisition). Three-dimensional images were obtained with water-excitation true fast imaging with steady-state precession (FISP) in the coronal plane (13/5; flip angle, 28°; section thickness, 1.7 mm; gap, 20%; field of view, 512 × 256 mm; matrix size, 384 × 235; voxel size, 0.5 × 0.3 × 1.7 mm; one acquisition). Imaging covered the area from 5 cm proximal to the radiohumeral joint space to the radial tuberosity.

Analysis of MR Images

Images were evaluated independently by three radiologists (reader 1: N.S., with 5 years of experience in musculoskeletal MR imaging; reader 2: D.B.H., with 2 years of experience in musculoskeletal MR imaging; reader 3: M.Z., with 15 years of experience in musculoskeletal MR imaging). The complete set of images from each volunteer was presented to the readers in a random fashion during an 8-week period. Qualitative image evaluation was performed by all three readers, and quantitative image evaluation was performed by readers 1 and 2.

Qualitative Evaluation

The three readers independently evaluated the elbow ligaments (anterior UCL, posterior UCL, RCL, lateral UCL, and AL) for their visibility (completely visible, partially visible [when the ligament could not be followed throughout its entire course], or not visible), their signal intensity with fluid-sensitive sequences (normal low signal intensity or increased signal intensity, hyperintense to surrounding muscle), and their signal intensity pattern (homogeneous, striated). Increased signal intensity between the normal ligament fibers was classified as striation, and increased signal intensity within or across the fibers was referred to as increased signal intensity. Readers 1 and 2 subjectively identified the sequence and plane that provided the best depiction of each ligament. The presence of a posterolateral plica (a meniscoid structure between the radial head and the capitellum also referred to as the humeroradial synovial fold), a posterior plica (a similar structure in the posterolateral olecranon recess adjacent to the anconeus muscle), and a pseudodefect of the capitellum (defined as a discontinuation of the osseous cortex) was assessed.

Figure 1

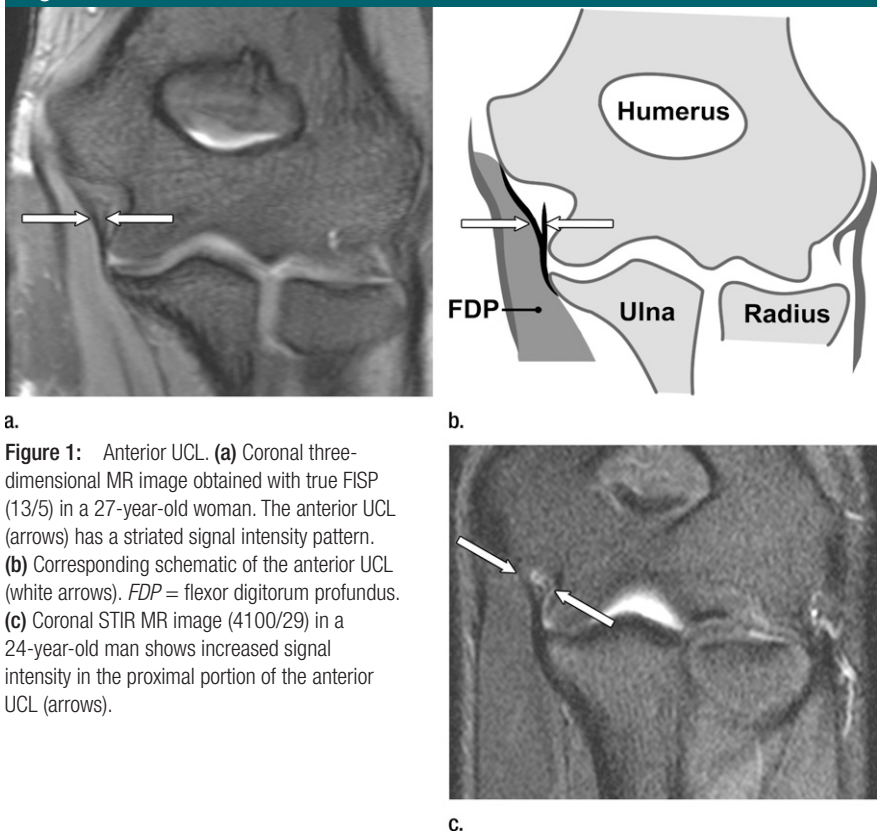

Figure 1: Anterior UCL. **(a)** Coronal three-dimensional MR image obtained with true FISP (13/5) in a 27-year-old woman. The anterior UCL (arrows) has a striated signal intensity pattern. **(b)** Corresponding schematic of the anterior UCL (white arrows). *FDP* = flexor digitorum profundus. **(c)** Coronal STIR MR image (4100/29) in a 24-year-old man shows increased signal intensity in the proximal portion of the anterior UCL (arrows).

Quantitative Evaluation

The thickness of the ligaments was measured by using a picture archiving and communication system workstation (ProVision PACS; Cerner, Kansas City, Mo), and measurements were obtained to the nearest one-tenth of a millimeter. All measurements were performed at the middle of each ligament by using images from the sequence that was determined to provide the best depiction of the ligament at qualitative evaluation (Figs 1–5).

All measurements were performed with electronic calipers. The size of the posterolateral plica (Fig 6) was measured in three dimensions (sagittal and craniocaudal on a sagittal image and mediolateral on a coronal image). The size of the posterior plica (Fig 7) in the posterolateral olecranon recess vis-à-vis the anconeus muscle was measured in two dimensions (sagittal and mediolateral)

Figure 2

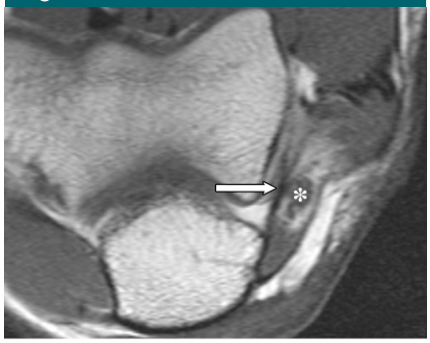

a.

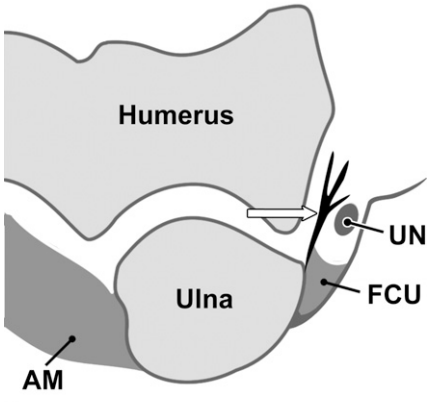

b.

Figure 2: Posterior UCL. **(a)** Transverse T1-weighted MR image (475/11) in a 33-year-old woman and **(b)** corresponding schematic show the posterior UCL (arrow) as well as the ulnar nerve (*UN*, asterisk in **a**). *AM* = anconeus muscle, *FCU* = flexor carpi ulnaris muscle.

Figure 3

a.

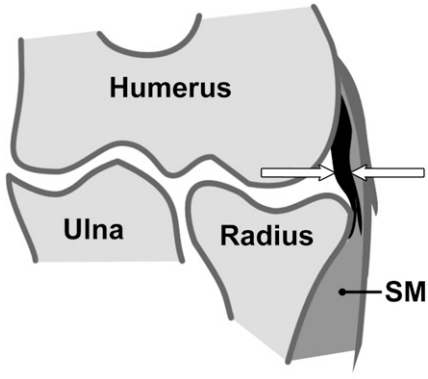

b.

Figure 3: RCL. **(a)** Coronal STIR MR image (4100/29) in a 28-year-old man. The RCL has a homogeneous appearance (arrows). **(b)** Corresponding schematic of the RCL (arrows). *SM* = supinator muscle.

on a transverse image. The pseudodefect of the capitellum (Fig 6c) was measured in two dimensions (sagittal on a sagittal image and mediolateral on a coronal image).

Statistical Analysis

The visibility of the ligaments, the presence of high signal intensity in the ligaments on fluid-sensitive images, and the presence of striations were noted independently by all three readers. Ranges and 25th, 50th, 75th, and 90th percentiles were calculated for the quantitative data obtained by readers 1 and 2. The relationships between the qualitative data obtained by reader 1 (visibility, high signal intensity on fluid-sensitive images, and striation) to age and sex were analyzed with the Kruskal-Wallis test and the Wilcoxon rank sum test, respectively. The Spearman rank correlation was used to assess the relationships between ligament and plicae thickness and age. The Pearson correlation was calculated to assess the relationship between qualitative results and height, weight, and body mass index. For all data, a P value of less than .05 was considered indicative of a statistically significant difference. Quantification of the interobserver agreement on the qualitative data was performed with κ statistics. The correlation coefficient was calculated to quantify the interobserver agreement on the quantitative data. According to Landis and Koch (33) a value of 0–0.20 is indicative of slight agreement, 0.21–0.40 fair agreement, 0.41–0.60 moderate agreement, 0.61–0.80 substantial agreement, and 0.81–1.00 almost-perfect agreement. A computer software package (SPSS, version 15; SPSS, Chicago, Ill) was used for all statistical calculations.

Results

Qualitative Analysis

A summary of the qualitative findings of all three readers is shown in Tables 1 and 2; the following results were derived from reader 1. The anterior UCL and RCL were completely visible in all 60 subjects (100%), whereas the posterior UCL, lateral UCL, and AL were completely visible in 58 (97%), 51 (85%), and 59 (98%) subjects, respectively, and partially visible in two subjects (3%), nine subjects (15%), and one subject (2%), respectively.

Increased signal intensity with fluid-sensitive sequences was seen in the anterior UCL (Fig 1c) in nine of the 60 subjects (15%), in the lateral UCL (Fig 4d) in six subjects (10%), in the posterior UCL in four subjects (7%), and in the RCL and AL in one subject each (2%). The remaining ligaments had normal signal intensity on fluid-sensitive images.

Striation was most commonly seen in the anterior UCL (Fig 1a) (52 of 60 subjects, 87%), followed by the lateral UCL (47 of 60 subjects, 78%) and the posterior UCL and AL (17 of 60 subjects for each, 28%); striation was least common in the RCL (six of 60 subjects, 10%). A homogeneous signal intensity pattern was found in the remaining ligaments (Fig 3a).

The posterolateral plica (Fig 6) was seen in 59 of the 60 subjects (98%), and the posterior plica (Fig 7) was seen in 20 (33%). A pseudodefect of the capitellum (Fig 6e) was noted in 51 of the 60 subjects (85%).

Quantitative Analysis

The median ligament thickness was 2.5 mm (range, 0.9–4.3 mm) for the anterior UCL, 1.0 mm (range, 0.5–2.2 mm) for the posterior UCL, 1.9 mm (range, 1.2–4.2 mm) for the RCL, 2.3 mm (range,

Figure 4

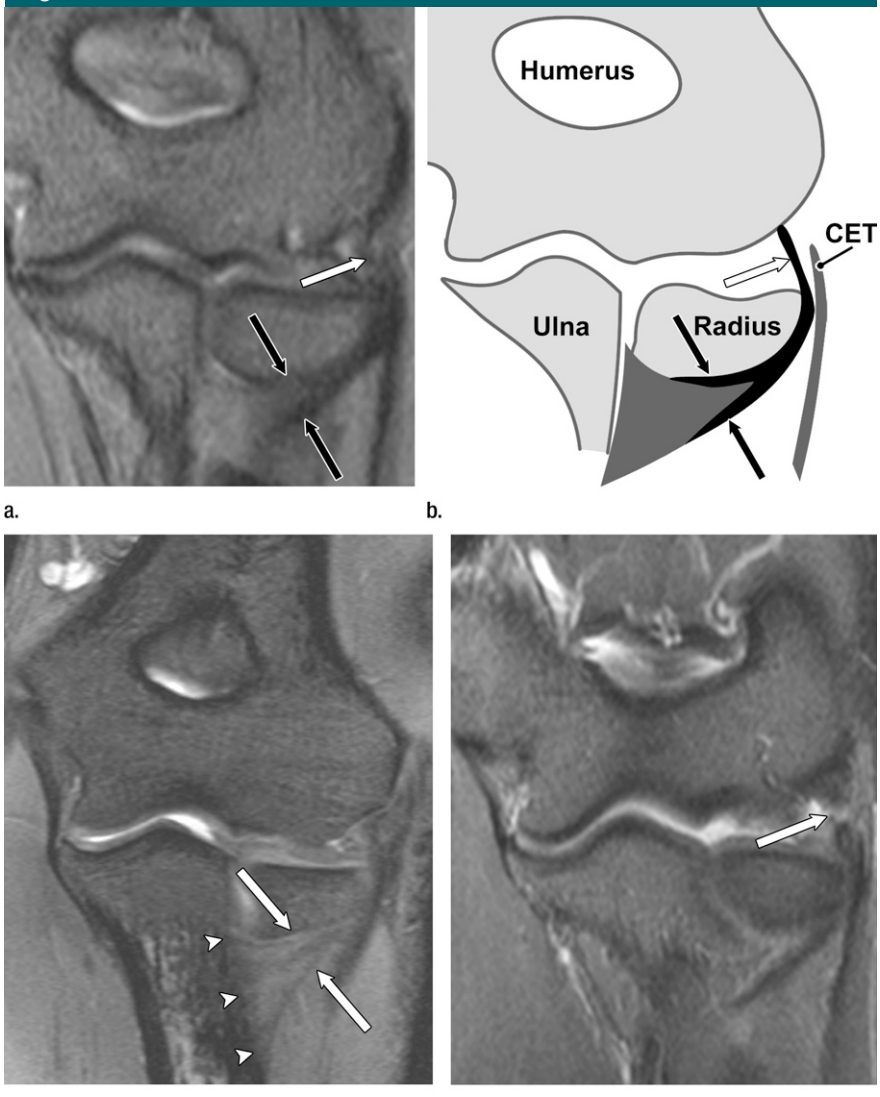

Figure 4: Lateral UCL. **(a)** Coronal STIR MR image (4100/29) in a 27-year-old woman. There is normal signal intensity in the proximal (white arrow) and distal (black arrows) aspects of the lateral UCL. **(b)** Corresponding schematic of the lateral UCL shows the proximal (white arrow) and distal (black arrows) aspects. *CET* = common extensor tendon. **(c)** Coronal three-dimensional MR image obtained with true FISP (13/5) in a 32-year-old man. The lateral UCL (arrows) has a striated signal intensity pattern and a broad attachment to the supinator crest of the ulna (arrowheads). **(d)** Coronal STIR MR image (4100/29) in a 49-year-old man shows increased signal intensity in the proximal portion of the lateral UCL (arrow).

Figure 5

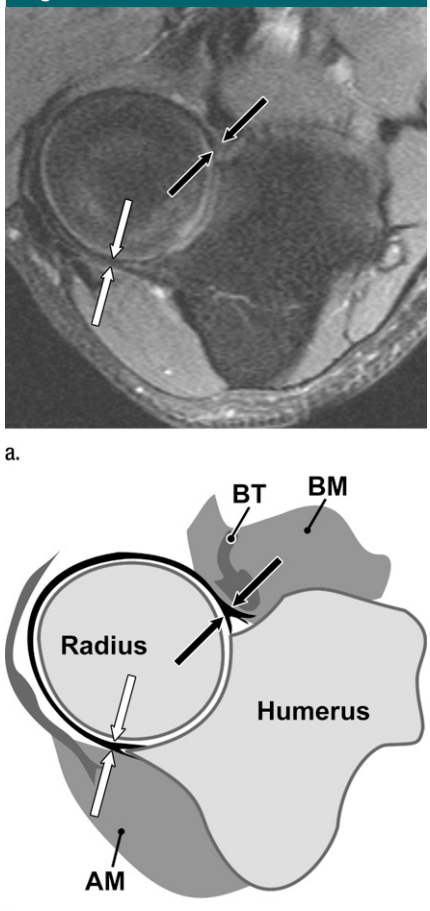

Figure 5: AL. **(a)** Transverse intermediate-weighted fat-suppressed MR image (3000/38) in a 40-year-old man demonstrates the posterior (white arrows) and anterior (black arrows) attachment of the AL to the radial notch and its course around the radial head. **(b)** Corresponding schematic of the AL shows the posterior (white arrows) and anterior (black arrows) attachments of the AL to the radial notch. *AM* = anconeus muscle, *BM* = brachialis muscle, *BT* = brachialis tendon.

1.3–4.8 mm) for the lateral UCL, and 1.0 mm (range, 0.5–1.5 mm) for the AL. The 90th percentile was 3.5 mm for the anterior UCL, 1.7 mm for the posterior UCL, 2.8 mm for the RCL, 3.8 mm for the lateral UCL, and 1.3 mm for the AL.

The median size of the posterolateral plica was 4.3 × 1.9 × 3.9 mm (sagittal × craniocaudal × mediolateral dimensions), and the median size of the posterior plica was 1.8 × 1.4 mm (sagittal × mediolateral dimensions). The 90th percentile for the craniocaudal dimension of the posterolateral plica was 2.6 mm, and that for the mediolateral dimension of the posterior plica was 2.0 mm.

The median size of the pseudodefect was 3.3 × 5.6 mm (sagittal × mediolateral dimensions; range, 1.9–7.4 × 1.1–9.5 mm). See Table 3 for details of the quantitative analysis performed by readers 1 and 2.

Statistical Analysis

Subjects with a striated signal intensity pattern in the lateral UCL were significantly younger than those without a striated signal intensity pattern in the lateral UCL (median age, 31.5 years vs 43.7 years, respectively; $P = .026$). A striated

Figure 6

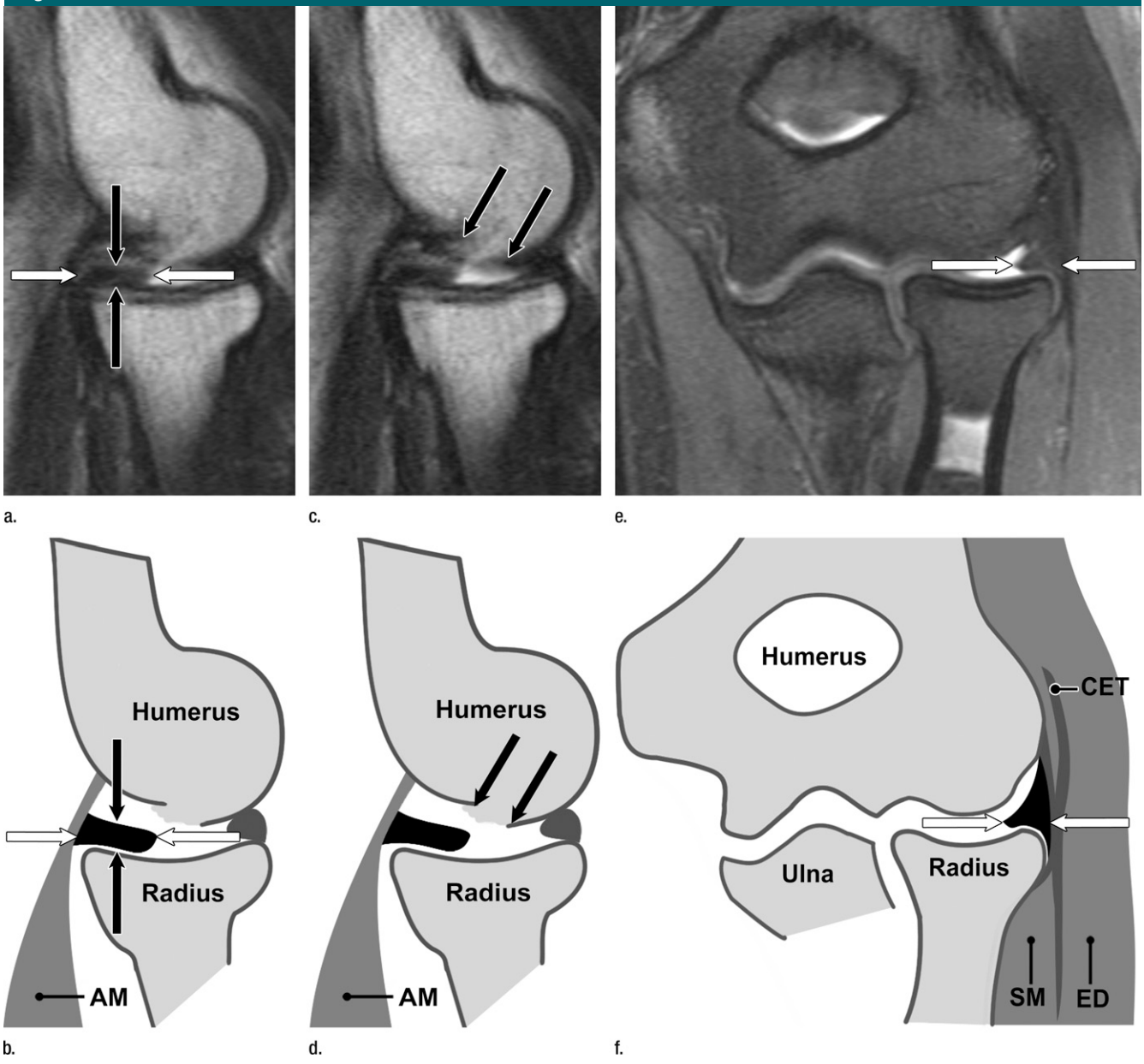

Figure 6: Posterolateral plica. **(a)** Sagittal T2-weighted MR image (3500/88) in a 33-year-old woman and **(b)** corresponding schematic demonstrate the anteroposterior (white arrows) and craniocaudal (black arrows) dimensions of the posterolateral plica. *AM* = anconeus muscle. **(c)** The same image as in **a** and **(d)** corresponding schematic demonstrate the pseudodefect of the capitellum (arrows) and its close relationship to the posterolateral plica. *AM* = anconeus muscle. **(e)** Coronal three-dimensional MR image obtained with true FISP (13/5) in the same volunteer and **(f)** corresponding schematic show the lateral aspect of the posterolateral plica (arrows). *CET* = common extensor tendon, *ED* = extensor digitorum muscle, *SM* = supinator muscle.

signal intensity pattern in the lateral UCL and AL was significantly more common in men (lateral UCL, $n = 27$; AL, $n = 12$) than in women (lateral UCL, $n = 20$; AL, $n = 5$) ($P = .028$ and .045, respectively).

The craniocaudal dimension of the posterolateral plica was significantly larger in men than in women (median, 2.1 mm vs 1.9 mm, respectively; $P = .036$). The mediolateral dimension of the pseudodefect of the capitellum was significantly larger in men than in women (median, 5.9 mm vs 5.0 mm, respectively; $P = .033$). A positive correlation was found between weight and the thickness of the anterior UCL ($r = 0.48$, $P < .001$), between height and the thickness of the anterior UCL ($r = 0.55$, $P < .001$), and between height and the thickness of the RCL ($r = 0.29$, $P < .05$). There was no correlation between height, weight, or

Figure 7

a.

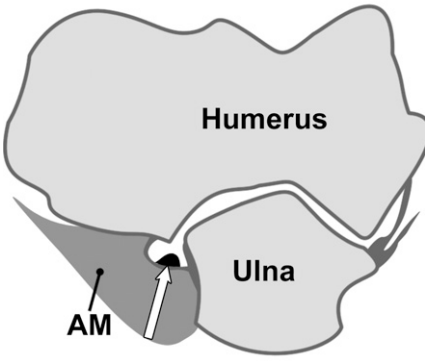

b.

Figure 7: Posterior plica. **(a)** Transverse intermediate-weighted fat-suppressed MR image (3000/38) in a 26-year-old man and **(b)** corresponding schematic show the posterior plica (arrow). *AM* = anconeus muscle.

body mass index and all other quantitative data.

The intraclass correlation coefficients for the quantitative measurements of the ligaments, plicae, and pseudodefects ranged from 0.274 to 0.882. Observer agreement on qualitative data ranged from 0.233 to 1.0.

No relationship between age and the thickness of the elbow ligaments, the size of the plicae, or the size of the pseudodefect was found.

Discussion

The ligaments of the elbow are often completely visible with conventional MR imaging sequences. In our study, however, the lateral UCL was only partially visible (not visible over the entire course) in one-sixth of the examined asymptomatic subjects. The visibility of the lateral

Table 1

Qualitative Evaluation of the Elbow Ligaments

	UCL				
Parameter and Reader	Anterior	Posterior	Lateral	RCL	AL
Visibility*					
Completely visible					
Reader 1	100 (60)	97 (58)	85 (51)	100 (60)	98 (59)
Reader 2	100 (60)	97 (58)	82 (49)	97 (58)	98 (59)
Reader 3	100 (60)	100 (60)	77 (46)	100 (60)	98 (59)
Agreement†	1.0	0.23	0.46	0.99	0.32
Partially visible					
Reader 1	0 (0)	3 (2)	15 (9)	0 (0)	2 (1)
Reader 2	0 (0)	3 (2)	18 (11)	3 (2)	2 (1)
Reader 3	0 (0)	0 (0)	23 (14)	0 (0)	2 (1)
Agreement†	1.0	0.23	0.46	0.98	0.32
Signal intensity with fluid-sensitive sequences					
Normal/low					
Reader 1	85 (51)	93 (56)	90 (54)	98 (59)	98 (59)
Reader 2	87 (52)	97 (58)	88 (53)	88 (53)	98 (59)
Reader 3	87 (52)	97 (58)	85 (51)	95 (57)	98 (59)
Agreement†	0.91	0.74	0.38	0.42	1.0
Increased					
Reader 1	15 (9)	7 (4)	10 (6)	2 (1)	2 (1)
Reader 2	13 (8)	3 (2)	12 (7)	12 (7)	2 (1)
Reader 3	13 (8)	3 (2)	15 (9)	5 (3)	2 (1)
Agreement†	0.91	0.74	0.38	0.42	1.0
Signal intensity pattern					
Homogeneous					
Reader 1	13 (8)	72 (43)	22 (13)	90 (54)	72 (43)
Reader 2	8 (5)	77 (46)	17 (10)	72 (43)	78 (47)
Reader 3	13 (8/60)	77 (46)	18 (11)	82 (49)	77 (46)
Agreement†	0.73	0.91	0.82	0.53	0.88
Striated					
Reader 1	87 (52)	28 (17)	78 (47)	10 (6)	28 (17)
Reader 2	92 (55)	23 (14)	83 (50)	28 (17)	22 (13)
Reader 3	87 (52)	23 (14)	82 (49)	18 (11)	23 (14)
Agreement†	0.73	0.91	0.82	0.53	0.88
Best imaging sequence and plane‡					
STIR coronal					
Reader 1	17 (10)	0 (0)	77 (46)	77 (46)	0 (0)
Reader 2	12 (7)	0 (0)	55 (33)	67 (40)	0 (0)
3D FISP coronal					
Reader 1	83 (50)	0 (0)	23 (14)	23 (14)	0 (0)
Reader 2	88 (53)	0 (0)	45 (27)	33 (20)	0 (0)
Intermediate-weighted FS transverse					
Reader 1	0 (0)	27 (16)	0 (0)	0 (0)	80 (48)
Reader 2	0 (0)	28 (17)	0 (0)	0 (0)	88 (53)

Table 1 (continues)

Table 1 (Continued)

Qualitative Evaluation of the Elbow Ligaments

Parameter and Reader	UCL			RCL	AL
	Anterior	Posterior	Lateral		
T1-weighted SE transverse					
Reader 1	0 (0)	73 (44)	0 (0)	0 (0)	20 (12)
Reader 2	0 (0)	72 (43)	0 (0)	0 (0)	12 (7)
Agreement†	0.56	0.71	0.62	0.76	0.57

Note.—Except for the analysis of the best imaging sequence and plane, qualitative analyses were performed by three independent readers. Data were obtained in 60 subjects. Except where indicated, data are given as percentages. Numbers in parentheses are numbers of subjects.

* All ligaments were either completely or partially visible.

† Data are κ values.

‡ FS = fat saturated, SE = spin echo, 3D FISP = three-dimensional water-excitation true FISP.

Table 2

Qualitative Evaluation of Plicae and Pseudodefects of the Elbow

Finding and Reader	Plica		Pseudodefect
	Posterolateral	Posterior	
Present			
Reader 1	98 (59)	33 (20)	85 (51)
Reader 2	100 (60)	32 (19)	85 (51)
Reader 3	98 (59)	30 (18)	87 (52)
Agreement*	0.99	0.56	0.96
Not present			
Reader 1	2 (1)	67 (40)	15 (9)
Reader 2	0 (0)	68 (41)	15 (9)
Reader 3	2 (1)	70 (42)	13 (8)
Agreement*	0.99	0.56	0.96

Note.—Data are from three independent readers and were obtained in 60 subjects. Except where indicated, data are given as percentages. Numbers in parentheses are numbers of subjects.

* Data are κ values.

UCL was nevertheless better than that reported previously in cadaver and MR imaging studies (11,17). In 1985, Morrey and An (11) found an "invariably present but often inconspicuous portion of the lateral complex consisting of a structure that inserts on a tubercle of the supinator crest" in five of 10 (50%) fresh-frozen upper extremity specimens and named it the *lateral ulnar collateral ligament*. The lateral UCL is the most important posterolateral stabilizer of the elbow joint (11,34). In an MR study, Terada et al (17) identified the lateral UCL as a clearly hypointense structure in 10 of 20 asymptomatic elbows (50%). The findings in the remaining 50% of elbows were ambiguous. The large number of lateral UCLs that were completely visible in our study might have been due to reader bias because the readers were aware that the imaged elbows were asymptomatic.

The frequently striated appearance of the anterior and lateral UCLs was an unexpected finding of our study. The other ligaments had a more homogeneous appearance. The striation was more prevalent in younger subjects than in older subjects. This tendency for normal striation in ligaments of younger individuals was previously seen in an MR imaging study of asymptomatic ankle ligaments (35). Mengiardi et al (35) found that a younger age was significantly associated with striation of the posterior tibiotalar ligament. In that study, the posterior tibiotalar ligament in all subjects younger than 45 years had a striated appearance; striation was often absent in older subjects. Further studies are needed to determine whether the absence of striation in the anterior and lateral UCLs can be considered a sign of degeneration or another abnormality.

Several plicae can be found throughout the elbow joint. We evaluated the most commonly addressed plicae in the literature: the posterolateral plica of the humeroradial joint and the posterior plica in the olecranon recess vis-à-vis the anconeus muscle. Thickening of these plicae induced by aging, chronic injuries, or inflammation has been related to symptoms (18–21). The high prevalence of a posterolateral plica in asymptomatic subjects (98%) suggests that the mere presence of a posterolateral plica may not explain clinical symptoms. The size of the plica should be taken into account. In the literature, it has been shown that there is an overlap in size between symptomatic and asymptomatic plicae (18). In our study, the craniocaudal dimension of the posterolateral plica in asymptomatic elbows never exceeded 3.1 mm. In the tested age group, thickening of the posterolateral plica should be diagnosed only when it is greater than 3 mm.

Duparc et al (20) dissected 50 elbows of adult cadavers and found a posterolateral plica to be present in 43 (86%), which is slightly lower than the prevalence in our study (98%, 59 of 60 asymptomatic subjects).

Awaya et al (18) evaluated the superior, medial, and lateral olecranon recess as well as the anterior humeral recess. They found a posterior plica in the lateral olecranon recess on conventional MR images of nonlocking elbows in 43 of 153 cases (28%). A posterior plica was found in the same location in eight of 11 cases (73%) at MR arthrography of nonlocking elbows. In our study, we used conventional MR images and found a posterior plica in the lateral olecranon recess to be

Table 3

Summary of Ligament, Plica, and Pseudodefect Sizes

Parameter and Reader	Percentile*				Range*	Standard Deviation*	Intraclass Correlation Coefficient
	25th	50th	75th	90th			
Anterior UCL							
Reader 1	2.0	2.5	3.0	3.5	0.9–4.3	0.70	
Reader 2	2.0	2.5	3.0	3.8	1.4–4.2	0.75	0.843
Posterior UCL							
Reader 1	0.8	1.0	1.2	1.7	0.5–2.2	0.35	
Reader 2	1.0	1.0	1.5	2.0	0.6–2.4	0.42	0.54
RCL							
Reader 1	1.7	1.9	2.2	2.8	1.2–4.2	0.55	
Reader 2	1.9	2.0	2.7	3.0	1.6–4.1	0.58	0.495
Lateral UCL							
Reader 1	2.0	2.3	3.2	3.8	1.3–4.8	0.89	
Reader 2	2.0	2.4	3.4	4.0	1.1–5.0	0.92	0.642
AL							
Reader 1	0.9	1.0	1.2	1.3	0.5–1.5	0.22	
Reader 2	1.0	1.2	1.3	1.5	0.7–2.0	0.25	0.405
Posterolateral plica							
Sagittal							
Reader 1	3.4	4.3	5.5	6.8	1.6–7.3	1.49	
Reader 2	2.8	4.0	5.0	6.8	1.5–8.0	1.63	0.702
Craniocaudal							
Reader 1	1.7	1.9	2.3	2.6	1.0–3.1	0.52	
Reader 2	1.9	2.1	3.1	4.3	1.0–6.7	1.2	0.274
Mediolateral							
Reader 1	3.0	3.9	5.5	6.3	1.0–7.7	1.53	
Reader 2	3.1	4.0	5.4	6.8	1.2–7.1	1.55	0.871
Posterior plica							
Sagittal							
Reader 1	1.1	1.8	2.8	3.2	0.8–4.8	1.01	
Reader 2	1.1	2.0	2.5	3.0	1.0–5.0	1.00	0.822
Mediolateral							
Reader 1	0.9	1.4	1.7	2.0	0.3–2.6	0.54	
Reader 2	1.0	1.7	2.0	2.9	0.5–4.0	0.81	0.510
Pseudodefect							
Sagittal							
Reader 1	2.6	3.3	4.2	4.8	1.9–7.4	1.17	
Reader 2	3.0	4.0	4.6	5.8	1.8–7.4	1.33	0.844
Coronal							
Reader 1	4.7	5.6	6.8	8.0	1.1–9.5	1.65	
Reader 2	5.0	5.9	7.0	8.1	1.0–10.6	1.78	0.822

Note.—Data are from two independent readers.

* Data are given in millimeters.

present in a similar percentage of cases (33%, 20 of 60 subjects). In the study by Duparc et al (20), the mean maximal thickness (craniocaudal dimension) of the posterolateral plica in cadavers was 1.7 mm (range, 1–4 mm), which is similar to that in our study (median thickness, 1.9 mm; range, 1.0–3.1 mm; 90th percentile, 2.6 mm). In the study by Awaya et al (18), none of the posterior plicae seen in the lateral olecranon recess were thicker than 3 mm; this correlates with our findings for the posterior plica (median thickness [mediolateral dimension], 1.4 mm; range, 0.3–2.6 mm; 90th percentile, 2.0 mm).

The MR imaging appearance of pseudodefects of the capitellum was first described by Rosenberg et al (22) in 1994. The pseudodefect of the capitellum is located close to the posterolateral plica. Therefore, we evaluated the prevalence and size of the pseudodefect of the capitellum when we addressed the ligaments and plicae in our study. In 1966, Osborne and Cotterill (24) reported on recurrent dislocation of the elbow and described "an osteochondral fracture in the posterolateral margin of the capitellum with or without a crater or shovel-like defect in the radial head" as the main abnormality of this condition. One can assume that the fracture in the posterolateral aspect of the capitellum may be minimal in some cases. In such a condition, it may be difficult to differentiate between a contusion of a normal pseudodefect or a real posttraumatic osteochondral defect (23). Rosenberg et al (22) found a pseudodefect in 36 of 54 patients and asymptomatic volunteers (66%). In our study, a pseudodefect was seen in 51 of the 60 volunteers (85%). The lower pseudodefect rate in the study by Rosenberg et al (22) can be explained by the fact that imaging planes were not always truly parallel and perpendicular to the humeral epicondyles, which usually resulted in images with a less conspicuous or absent pseudodefect. It is important to differentiate a pseudodefect of the capitellum from clinically relevant findings, including Panner disease, osteochondritis dissecans, and acute traumatic impaction injuries of the capitellum (25–30). To our knowledge, the normal size of a pseudodefect has not yet been reported in the literature. On the basis of our 90th percentile data, we have shown that a pseudodefect measuring up to 5 × 8 mm (sagittal × mediolateral dimensions) can be considered normal.

In our study, the observers were aware of the fact that all elbows were asymptomatic, and this may have had an effect on the qualitative assessments. However, the facts that all ligaments could be measured and appropriate κ values were obtained in the interobserver agreement test (0.48–1.00) indicate that the reading of the images was robust.

Accepting this limitation, we conclude that elbow ligaments and the posterolateral plica can be seen on conventional MR images in most asymptomatic subjects. Most asymptomatic ligaments are thinner than 4 mm, and most plicae are thinner than 3 mm. The anterior and lateral UCLs usually have a striated appearance on MR images. We have provided quantitative values that may be useful for evaluating symptomatic elbows.

Acknowledgments: We thank Tallal C. Mamisch, MD, and Samuel Richard, PhD, for their support with the data analysis.

References

1. Beckett KS, McConnell P, Lagopoulos M, Newman RJ. Variations in the normal anatomy of the collateral ligaments of the human elbow joint. J Anat 2000;197(pt 3):507–511.
2. Carrino JA, Morrison WB, Zou KH, Steffen RT, Snearly WN, Murray PM. Lateral ulnar collateral ligament of the elbow: optimization of evaluation with two-dimensional MR imaging. Radiology 2001;218(1):118–125.
3. Carrino JA, Morrison WB, Zou KH, Steffen RT, Snearly WN, Murray PM. Noncontrast MR imaging and MR arthrography of the ulnar collateral ligament of the elbow: prospective evaluation of two-dimensional pulse sequences for detection of complete tears. Skeletal Radiol 2001;30(11):625–632.
4. Cotten A, Jacobson J, Brossmann J, et al. Collateral ligaments of the elbow: conventional MR imaging and MR arthrography with coronal oblique plane and elbow flexion. Radiology 1997;204(3):806–812.
5. Fowler KA, Chung CB. Normal MR imaging anatomy of the elbow. Radiol Clin North Am 2006;44(4):553–567, viii.
6. Kaplan LJ, Potter HG. MR imaging of ligament injuries to the elbow. Radiol Clin North Am 2006;44(4):583–594, ix.
7. Kijowski R, Tuite M, Sanford M. Magnetic resonance imaging of the elbow. II. Abnormalities of the ligaments, tendons, and nerves. Skeletal Radiol 2005;34(1):1–18.
8. Ly JQ, Sanders TG, Beall DP. MR imaging of the elbow: a spectrum of common pathologic conditions. Clin Imaging 2005;29(4):278–282.
9. Melloni P, Valls R. The use of MRI scanning for investigating soft-tissue abnormalities in the elbow. Eur J Radiol 2005;54(2):303–313.
10. Moritomo H, Murase T, Arimitsu S, Oka K, Yoshikawa H, Sugamoto K. The in vivo isometric point of the lateral ligament of the elbow. J Bone Joint Surg Am 2007;89(9):2011–2017.
11. Morrey BF, An KN. Functional anatomy of the ligaments of the elbow. Clin Orthop Relat Res 1985;(201):84–90.
12. Munshi M, Pretterklieber ML, Chung CB, et al. Anterior bundle of ulnar collateral ligament: evaluation of anatomic relationships by using MR imaging, MR arthrography, and gross anatomic and histologic analysis. Radiology 2004;231(3):797–803.
13. Nakanishi K, Masatomi T, Ochi T, et al. MR arthrography of elbow: evaluation of the ulnar collateral ligament of elbow. Skeletal Radiol 1996;25(7):629–634.
14. Rosenberg ZS, Bencardino J, Beltran J. MR imaging of normal variants and interpretation pitfalls of the elbow. Magn Reson Imaging Clin N Am 1997;5(3):481–499.
15. Timmerman LA, Schwartz ML, Andrews JR. Preoperative evaluation of the ulnar collateral ligament by magnetic resonance imaging and computed tomography arthrography: evaluation in 25 baseball players with surgical confirmation. Am J Sports Med 1994;22(1):26–31, discussion 32.
16. van Kollenburg JA, Brouwer KM, Jupiter JB, Ring D. Magnetic resonance imaging signal abnormalities in enthesopathy of the extensor carpi radialis longus origin. J Hand Surg Am 2009;34(6):1094–1098.
17. Terada N, Yamada H, Toyama Y. The appearance of the lateral ulnar collateral ligament on magnetic resonance imaging. J Shoulder Elbow Surg 2004;13(2):214–216.
18. Awaya H, Schweitzer ME, Feng SA, et al. Elbow synovial fold syndrome: MR imaging findings. AJR Am J Roentgenol 2001;177(6):1377–1381.
19. Clarke RP. Symptomatic, lateral synovial fringe (plica) of the elbow joint. Arthroscopy 1988;4(2):112–116.
20. Duparc F, Putz R, Michot C, Muller JM, Fréger P. The synovial fold of the humeroradial joint: anatomical and histological features, and clinical relevance in lateral epicondylalgia of the elbow. Surg Radiol Anat 2002;24(5):302–307.
21. Steinert AF, Goebel S, Rucker A, Barthel T. Snapping elbow caused by hypertrophic synovial plica in the radiohumeral joint: a report of three cases and review of literature. Arch Orthop Trauma Surg 2010;130(3):347–351.
22. Rosenberg ZS, Beltran J, Cheung YY. Pseudodefect of the capitellum: potential MR imaging pitfall. Radiology 1994;191(3):821–823.
23. Jeon IH, Micic ID, Yamamoto N, Morrey BF. Osborne-Cotterill lesion: an osseous defect of the capitellum associated with instability of the elbow. AJR Am J Roentgenol 2008;191(3):727–729.
24. Osborne G, Cotterill P. Recurrent dislocation of the elbow. J Bone Joint Surg Br 1966;48(2):340–346.
25. Bowen RE, Otsuka NY, Yoon ST, Lang P. Osteochondral lesions of the capitellum in pediatric patients: role of magnetic resonance imaging. J Pediatr Orthop 2001;21(3):298–301.
26. Kijowski R, De Smet AA. MRI findings of osteochondritis dissecans of the capitellum with surgical correlation. AJR Am J Roentgenol 2005;185(6):1453–1459.
27. Marshall KW, Marshall DL, Busch MT, Williams JP. Osteochondral lesions of the humeral trochlea in the young athlete. Skeletal Radiol 2009;38(5):479–491.
28. Rosenberg ZS, Blutreich SI, Schweitzer ME, Zember JS, Fillmore K. MRI features of posterior capitellar impaction injuries. AJR Am J Roentgenol 2008;190(2):435–441.
29. Stoane JM, Poplausky MR, Haller JO, Berdon WE. Panner's disease: x-ray, MR imaging findings and review of the literature. Comput Med Imaging Graph 1995;19(6):473–476.
30. Rajeev A, Pooley J. Lateral compartment cartilage changes and lateral elbow pain. Acta Orthop Belg 2009;75(1):37–40.
31. Husarik DB, Saupe N, Pfirrmann CW, Jost B, Hodler J, Zanetti M. Elbow nerves: MR findings in 60 asymptomatic subjects—normal anatomy, variants, and pitfalls. Radiology 2009;252(1):148–156.
32. Morrey BF, ed. The elbow and its disorders. In: Functional evaluation of the elbow. 2nd ed. Philadelphia, Pa: Saunders, 1993; 86–89.
33. Landis JR, Koch GG. The measurement of observer agreement for categorical data. Biometrics 1977;33(1):159–174.
34. Dunning CE, Zarzour ZD, Patterson SD, Johnson JA, King GJ. Ligamentous stabilizers against posterolateral rotatory instability of the elbow. J Bone Joint Surg Am 2001;83-A(12):1823–1828.
35. Mengiardi B, Pfirrmann CW, Vienne P, Hodler J, Zanetti M. Medial collateral ligament complex of the ankle: MR appearance in asymptomatic subjects. Radiology 2007;242(3):817–824.